INTERACTION OF SPHERICAL SHOCK WAVE WITH BODIES

A. N. Ivanov and S. Yu. Chernyavskii

The basic results of shock wave interaction with bodies have been obtained experimentally in shock tubes which are characterized by constant flow parameters behind the wave, for example the studies of [1, 2]. In the present paper we examine the interaction between bodies and a spherical explosive wave which has essentially unsteady flow behind the compression shock. Measurements are made of the force impulse (time integral of the force) imparted by the explosive wave to a cylindrical stationary body, and studies are made of the flow pattern formation near a flying blunt body.

1. FORCE IMPULSE MEASUREMENTS

The spherical shock wave in the experiments was created by the explosion of a chemical explosive charge. The wave interacted with a circular cylinder supported freely by slender filaments perpendicular to the direction of propagation of the compression shock. Since the cylinder mass remained constant in the course of the experiment and the reactions of the supporting filaments in the direction of motion can be neglected, the magnitude of the force impulse at each moment of time is proportional to the velocity of the body. The instantaneous velocity values were determined by two methods: by electric integration over time of the signal from a piezoelectric accelerometer mounted on the body, and by the electromagnetic method.

A type IS-313 piezoelectric accelerometer having dimensions $16 \times 16 \times 19$ mm^3 and sensitivity 0.5 mV $\cdot$ sec^2/m was mounted at the center of the cylinder for the measurements using the first method. The sensor signal was fed through an antimicrophonic cable to the preamplifier input, was then integrated with respect to time by an integrating amplifier, and recorded on a dual-channel cathode ray oscillograph. The second oscillograph channel was used to record the signal from the piezoelectric sensor measuring the differential static pressure behind the explosive wave front [3]. The oscillograph was triggered by a synchronizing pressure pickup.

Prior to installing the accelerometer in the cylinder, the entire velocity measurement loop was calibrated uisng a pneumatic device consisting of a high-pressure chamber, a cylindrical tubing segment connected with the chamber, and a fast-acting electrically-operated valve which blocks air entry from the tubing into the chamber. A piston with a bracket for mounting the sensor being calibrated was installed in the tubing right next to the valve. When the valve is opened, the piston travels with uniform acceleration and its velocity at every instant is determined from the known values of the initial air pressure in the chamber, the piston cross-sectional area, and the mass of the piston together with the sensor.

The static pressure sensor was calibrated using a pulsed pneumatic device [4].

When installed in the cylinder, the accelerometer was centered by locking screws and potted with Wood's alloy with a melting point of 60°C. This technique made it possible to simplify assembly and disassembly of the sensor and to increase the sensor natural vibration frequency relative to the cylinder.

When using the electromagnetic method, the velocity sensor was the cylinder itself, fabricated from current-conducting material and placed in a constant magnetic field with intensity of about 150 Oe, uniform

Moscow. Translated from Zhurnal Prikladnoi Mekhaniki i Tekhnicheskoi Fiziki, Vol. 10, No. 6, pp. 115-119, November-December, 1969. Original article submitted January 6, 1969.

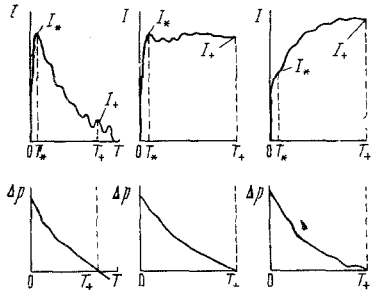

Fig. 1

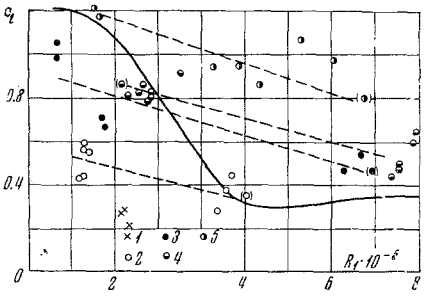

Fig. 2

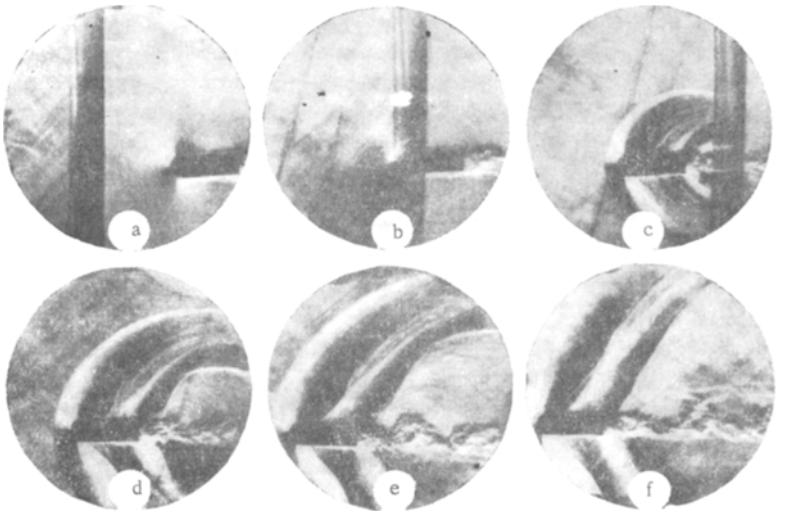

Fig. 3

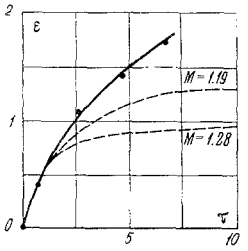

Fig. 4

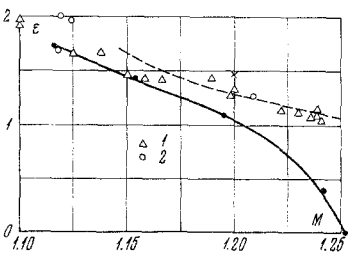

Fig. 5

in the shock wave motion direction. The field was created by en electromagnet with pole pieces of 10×200 mm^2 section, oriented toward the center of the explosion and equipped with fairings. Control measurements in the working zone between the poles, made using static and total pressure sensors [3], showed that the presence of the electromagnet has practically no effect on the nature of the flow behind the explosive wave front. Two slender rigid electrodes, oriented in the direction of its motion, were attached to the cylinder. The inductive emf appearing at the ends of the electrodes as the cylinder moves under the influence of the blast wave was recorded on the dual-channel cathode ray oscillograph. As in the first method, the other channel was used to record the signal from the piezoelectric static pressure sensor.

The calibration of the circuit for measuring velocity by the electromagnet method was accomplished using the pneumatic device described above. For this purpose the piston of the calibrating device was connected rigidly with the test cylinder, mounted directly in the test zone.

The overall force impulse measurement error using both of the methods described did not exceed 10%, and the static pressure measurement error did not exceed 3%.

The accelerometer was used to measure the force impulse imparted by the blast wave to cylinders with diameters D = 28 mm (length 210 mm) and D = 50 mm (length 300 mm). The electromagnetic method was used in studying the initial segment of the impulse curve for cylinders with diameters D = 28 mm (length 210 mm) and D = 10 mm (length 100 mm).

All the cylinders were tested at a fixed distance of 5.1 m from the blast center for initial air pressures $p_0 = 1.0$ and 0.3 kg/cm^2. The relative static pressure differential across the blast wave front was

$$\frac{\Delta p_1}{p_0} = \begin{cases} 0.25 - 1.1 \text{ for } p_0 = 1.0 \text{ kg/cm}^2 \\ 0.4 - 1.1 \text{ for } p_0 = 0.3 \text{ kg/cm}^2 \end{cases}$$

Typical oscillograms of the force impulse I as a function of time T, obtained by the cylinder for different shock wave parameters, are shown in Fig. 1a, b, c, together with the corresponding curves of the differential static pressure Δp. On the oscillograms we can identify the initial segment with rapid increase of the impulse, terminating with a maximum (Fig. 1a, b) or an inflection point (Fig. 1c). The values of the time and impulse corresponding to this point are denoted by T_* and I_*. The impulse rate of change subsequently decreases markedly. At the moment T_+ of termination of the blast wave compression phase, the magnitude of the impulse reaches the value I_+. We note that the scatter of the results exceeds considerably the measurement error, particularly for the quantity I_+. This can apparently be explained by the instability of the phenomenon being studied.

The magnitude of the time interval corresponding to the initial segment can be represented in dimensionless form $t_* = T_* c_1/D$, where c_1 is the sound speed at the shock wave front. In the cases studied, the quantity t_* is practically the same and on the average amounts to $t_* \approx 2.0$. Comparison of this value with the results of experiments on cylinder interaction with a plane shock wave [2] shows that the initial impulse growth segment corresponds basically to the process of shock wave front diffraction by the cylinder. The magnitude of the dimensionless force impulse imparted to the body at the moment t_* is also a constant quantity (within the limits of experimental data scatter)

$$i_* = \frac{I_* c_1}{\Delta p_2 DS} \approx 0.7$$

Here Δp_2 is the differential pressure for normal shock wave front reflection, calculated from the known values of p_0 and Δp_1; S is the cylinder frontal area.

The impulse variation for $T_* < T < T_+$ is determined basically by the action on the cylinder of two oppositely directed forces: the velocity head of the approaching unsteady gas stream, and the force owing to the presence of the negative gradient of the pressure and velocity of the gas in the blast wave. Therefore, the quantity I_+ may be less than, equal to, or larger than the quantity I_* (Fig. 1), depending on the flow regime.

It is interesting to compare the total impulse I_+ imparted to the body at the moment when the blast wave compression phase terminates with the velocity head impulse I_0 during the same time interval. Their ratio $I_+/I_0 = c_i$ can be regarded as an effective drag coefficient of the cylinder, averaged over the time T_+. As the basic parameters characterizing this coefficient we can take the Mach, Reynolds, and Strouhal numbers at the shock wave front

$$M_1 = u_1/c_1, \qquad R_1 = \rho_1 u_1 D/\mu_1, \qquad S_1 = T_+ u_1/D$$

where u_1, ρ_1, μ_1 are the velocity, density, and viscosity of the gas at the front, calculated from the relations for the normal compression shock. In the experiments the Mach number M_1 did not exceed 0.5. As is known ([5, 6], for example), the Mach number variation in this range for steady flow past a cylinder has very little effect on the Reynolds number dependence of the drag coefficient c_x (for $10^5 < R \leq 10^6$). Assuming that this is also valid in the unsteady case, we shall study the influence on the coefficient c_i of only the Reynolds and Strouhal numbers.

Figure 2 shows the values of the quantity c_i obtained in the present study and for comparison the drag coefficient of an infinitely long cylinder for steady-state flow [5] (solid curve) as a function of the Reynolds number. The velocity head impulse was determined with the aid of the results of [7].

All the experiments were broken down into groups with similar values of the Strouhal numbers: 1 ($S_1 \approx 2.5$), 2 ($4.5 \leq S_1 \leq 6.5$), 3 ($7.5 \leq S_1 \leq 9.5$), 4 ($10.5 \leq S_1 \leq 14$), 5 ($21 \leq S_1 \leq 26$). Averaged curves of $c_i = c_i(R_1)$

are plotted for each group of points (other than the group corresponding to $S_1 \approx 2.5$). We see from Fig. 2 that for $R_1 = \text{const}$ the effective drag coefficient of the cylinder increases with increase of the Strouhal number. For a constant Strouhal number c_i decreases with increase of the Reynolds number, just as in the steady flow case.

2. BOW WAVE FORMATION ON FLYING BODY

The spherical blast wave was created using the same technique as in Section 1. A body accelerated to the required speed by a gas gun traveled opposite the wave front. The gun consisted of a barrel, a high pressure chamber, and a fast-acting electrically-operated valve mounted between the chamber and barrel.

The shock wave-body interaction process was visualized using a type IAB-451 half-shadow schlieren instrument. The SFR-2M high-speed photorecorder (operating in the continuous scan mode), together with a generator providing a series of light flashes of 0.1 μsec duration and repetition rate up to 30 kHz, was used to obtain a sequential series of images.

In order to obtain movies of the process of flying body interaction with the blast wave, it is necessary to select the moment of explosive charge detonation and the moment of opening of the gas gun electric valve so that the body encounters the wave front in the field of view of the optical system, and so that the photorecorder mirror occupies a position which will ensure that the image falls on the movie film. To accomplish this the signal from the synchronizing unit of the SFR-2M camera, after amplifying and shaping, was fed to the input of the unit which controls the gas gun electrovalve so that the valve opened and the acceleration of the body was initiated. This same signal was fed through a delay line to trigger the unit which initiated the explosive charge. At the instant the shock wave approached the recording zone, the light flash generator began to operate, triggered by the piezoelectric synchronizing unit.

Figure 3 shows schlieren photographs of the interaction of the spherical air blast wave with a body flying in the direction opposite the wave front. The body was a cylinder with hemispherical nosetip and fabricated from polystyrene foam. The cylinder length was 50 mm, diameter 20 mm, and weight 0.7 g. The body velocity in the undisturbed air corresponded to $M = 0.82$. In the region of encounter of the compression shock with the flying body the excess static pressure at the wave front amounted to 1.2 kg/cm^2 with a duration of the compression phase of 3.5 msec. All the experiments were conducted at normal atmospheric pressure of 1.03 kg/cm^2. The time intervals between the photographs shown were 0.107 msec. The body velocity measurement error did not exceed 2%, the differential static pressure measurement error was less than 4%, and the time interval measurement error was less than 0.5%.

We see in the pictures the intense bow wave which forms as the body enters the flow behind the blast wave front. The region bounded by the bow wave expands rapidly in the course of time. At the same time there is an increase of the distance d from the foward stagnation point on the body to the bow shock. Figure 4 shows the values of this distance, referred to the nosetip blunting radius r, as a function of dimensionless time τ; in the figure $\varepsilon = d/r$, $\tau = \frac{1}{2}Tc_1/r$.

Here T is the time interval after encounter of the wave front with the body. Also shown is the dependence of ε on τ, obtained in experiments with a stationary sphere in a shock tube for similar Mach numbers of the flow behind the shock [8]. We note that for $\tau \leq 2$ the dependence of ε on τ for the moving blunted cylinder and the stationary sphere is practically the same. With increase of τ the distance from the bow wave to the body in the shock tube reaches a stationary value corresponding to the body shape and the approaching flow Mach number. The blast wave is characterized by continuous decrease of the gas velocity with time, as a result of which the Mach number M of the flow approaching the body decreases constantly and the bow wave standoff distance increases correspondingly. The dependence of ε on the local Mach number is represented by the solid curve in Fig. 5. The values of M were calculated from the data of [7] with account for the experimental values of the differential pressure across the wave front and the body velocity.

This same figure shows analogous relations for the case of steady flow past a sphere, obtained experimentally ([8] points 1, [9] points 2), and by calculation [10] (dashed curve), and also the value of ε for $M = 1.2$, found by A. I. Golubinskii for a body similar to that studied in the present investigation (the crosses).

The experimental results shown in Figs. 4 and 5 make it possible to conclude that the bow wave formation process in the case studied can be arbitrarily divided into two states: the first is essentially unsteady,

and the second is quasisteady. In the second stage the distance between the bow wave and the body at every instant of time for varying approaching flow Mach number is close to the value obtained for steady-state flow past the body. Transition of the first stage into the second stage begins at $\tau \approx 2$.

The authors wish to thank A. I. Golubinskii for permission to use his experimental data on steady-state flow past models.

LITERATURE CITED

1. Collection: Shock Tubes [Russian translation], Izd-vo inostr. lit., Moscow, 1962.
2. Collection: Aerophysical Studies of Supersonic Flows [in Russian], Nauka, Moscow-Leningrad, 1967.
3. S. Yu. Chernyavskii, "Device for measuring total and static pressure in unsteady gasdynamic flows," USSR patent no. 159667; Byulleten izobret. i tovarnykh znakov, no. 1, 1964.
4. A. N. Ivanov, S. Yu. Chernyavskii, and V. P. Borisovskaya, USSR patent no. 226913, Byulleten izobret. i tovarnykh znakov, no. 29, 1968.
5. L. Prandtl and O. G. Tietjens, Fundamentals of Hydro- and Aeromechanics [Russian translation], Izd-vo inostr. lit., 1951.
6. A. Ferri, "Influenza del numero di Reynolds ai grandi numeri di Mach," Atti di Guidonia, no. 67-69, 1942.
7. A. S. Fonarev and S. Yu. Chernyavskii, "Calculation of shock waves for explosion of spherical explosive charges in air," Izv. AN SSSR, MZhG [Fluid Dynamics], vol. 3, no. 5, 1968.
8. M. P. Syshchikova, M. K. Berezkina, and A. N. Semenov, "Bow shock wave standoff from sphere in argon and nitrogen at low supersonic Mach numbers," collection: Aerophysical Studies of Supersonic Flows [in Russian], Nauka, Moscow-Leningrad, 1967.
9. V. G. Maslennikov and A. M. Studenkov, "On the position of the bow shock wave for Mach numbers close to one," collection: Aerophysical Studies of Supersonic Flows [in Russian], Nauka, Moscow-Leningrad, 1967.
10. O. M. Belotserkovskii, A. Bulekbaev, M. M. Golomazov, V. G. Grudnitskii, V. K. Dushin, V. F. Ivanov, Yu. P. Lun'kin, F. D. Popov, G. M. Ryabinkov, T. Ya. Timofeeva, A. I. Tolstykh, V. N. Fomin, and V. F. Shugaev, "Supersonic gas flow past blunt bodies," Tr. VTs AN SSSR, Moscow, 1967.